

EXTENDING LBP AND CONVOLUTION-LIKE OPERATIONS ON THE MESH

Claudio Tortorici, Naoufel Werghi

Stefano Berretti

Khalifa University, Abu Dhabi, UAE

University of Florence, Florence, Italy

ABSTRACT

Extending the concept of texture to the geometry of a mesh manifold surface is an emerging topic in image processing. This concept is different from gluing images to the surface, but rather indicates the presence of relief patterns that locally change the surface geometry, showing some regular and repetitive pattern. In this paper, we propose an efficient and effective framework to address this novel task, which encompasses the convolution operation and the casting of a variety of Local Binary Pattern on the mesh manifold. Results show that our technique outperforms the existing state-of-the-art methods in the challenging task of relief patterns classification.

Index Terms— Relief patterns, mesh convolution, LBP

1. INTRODUCTION

Using mesh manifolds as input data, several studies addressed the problem of retrieving/classifying 3D shapes based on their similarities [1]. In most of the cases, synthetic models generated by ad-hoc software have been used, while reconstructed meshes have been considered more rarely. An even less investigated, but emerging problem, which is of interest, for its potential application in several contexts, is the classification of 3D relief patterns. As peculiar characteristic, the style of these patterns does not depend on the overall structure of the shape. They are rather characterized by some form of regularity and repeatability across the surface so that they can be regarded as the 3D geometric equivalent of textures in 2D images. Examples are knitted fabrics, artworks' patterns, artists' styles or natural structures like tree barks [2], rock types or engravings [3], *etc.* Modeling such bas-reliefs from 3D objects revealed attractive also in Computer Graphics [4, 5].

One interesting idea for processing relief patterns is regarding them as a sort of mesh equivalent of image textures (in the following, we will also refer to relief patterns as *geometric texture*). In the 2D image domain, many approaches have tried to characterize texture patterns by their repeatability, randomness and orientation [6]. The most practiced solutions extracted such information by using local descriptors that can be computed via some filtering operations, like Gabor [7], or Local Binary Pattern (LBP). In particular, LBP has been one of the most simple and widely spread local

texture descriptor as proposed for the first time by Ojala *et al.* [8]. Thanks to its simplicity and discriminative power, LBP has been successfully implemented in several different contexts. However, its application to mesh manifolds could not be achieved till a *mesh*-version was introduced by Werghi *et al.* [9, 10, 11].

In this paper, we target the problem of classifying geometric textures on the mesh surface by proposing a framework which is distinguished by the following original contributions: 1) Extending image-like filtering operations to the mesh manifold domain, introducing discrete and continuous convolution operator on the mesh; 2) Enabling the extension of numerous LBP variant to the mesh manifold; and 3) Application to the classification and Retrieving relief pattern over 3D shapes.

2. RELATED WORK

Retrieval and classification of relief patterns on 3D meshes is a quite recent area of investigation, with several potential applications. First works on this topic were presented by Werghi *et al.* [9, 10, 11], who proposed a framework for computing LBP on the mesh manifold and showcased its applicability on geometric texture retrieval for a small set of prototype meshes. Later on, following the release of the first relief pattern dataset in the SHREC'17 contest [12], a set of different approaches for addressing this problem have been presented. In the following, we give an overview of the most relevant methods participating in the SHREC'17 track (see also [12] for more details) and other recent proposals.

Limberger and Wilson [12] proposed a curvature-based Laplace Beltrami operator (KLBO) to describe the relief patterns of surfaces. Starting from the eigen-decomposition of the KLBO, they computed and encoded the Improved Wave Kernel Signature (IWKS) [13] using two different encoding schemes, namely, the Fisher Vector (FV) or the Super Vector (SV). Afterwards, they employed Euclidean distance between the two encodings as texture descriptor. Velasco-Forero and Fehri [12], proposed an image covariance descriptor from morphological transformation of local curvature estimation. In their method, curvature descriptors are projected to a 2D image, where a set of morphological operations produced 96 descriptor images grouped in a single covariance matrix. This latter one is used as surface signature.

More recently, Giachetti [14] proposed the Improved Fisher Vector (IFV) to encode local invariant features. First, feature values are mapped from 3D meshes to a 2D raster image, then IFV is used on the raster image to estimate the texture local feature. Several 3D features, like SIFT and patch curvatures, are extracted from the mesh and then mapped on a planar surface to obtain a 2D representation of the texture. Finally, Moscoso Thompson *et al.* [15], developed an LBP-based descriptor, called *edgeLBP*, that works on the mesh. They defined the LBP rings using sphere-surface intersection: spheres of different radii are centered at each mesh vertex; once the intersections between the concentric spheres and the mesh edges are obtained, they are ordered and interpolated to generate a sequence of 12 equidistant points for each intersecting contour. Curvature descriptors are estimated at these points and used afterwards to compute LBP descriptors.

3. IMAGE-LIKE OPERATIONS ON THE MESH

Many successful solutions for texture analysis and classification in the image domain apply some local operators by relying on the grid-like structure of the pixels. These operations include image filtering based on convolutional masks, *e.g.*, Gabor and Haar's Wavelets, discrete directional derivatives, like in the histogram of gradient (HOG) descriptor, or more texture oriented solutions, like the Local Binary Pattern (LBP). Our founding idea here is to propose a sort of analogy between operations performed in 2D on the image grid and on the surface of a mesh manifold, *i.e.*, a 2D surface embedded in a 3D space. This allows us to extend to the mesh domain a vast class of well known image operators, thus deriving a general framework, which is both effective and efficient.

To target the above goal, we start by the intuitive idea of defining a local ordered structure on the mesh, which can be regarded as the equivalent on the mesh manifold of the image grid. This idea was concretized first by Werghi *et al.* [16] with the Ordered Ring Facet (ORF). The ORF construction starts with adjacent f_{out} facets to a central facet f_c , and linearly derives an ordered ring (see Fig. 1a). Such linear process can be repeated for multiple radius r to get multiple rings, thus extending the coverage of the ordered area (see Fig. 1b-c). Since the first facet of each ring is aligned to the same axis, we can use such ordered structure as a polar grid, with polar coordinates identified by the ring r and a sample k in the ring.

Convolution on the mesh – The possibility to inherit the order from the ORF allows us to define a shift operator on the mesh. While in the image the adjacent pixels to a given one are given by the Cartesian coordinates derived by the grid structure of the image itself, with the ORF we use polar coordinates, *i.e.*, radius r and quantized angle θ . Therefore, the convolution between a mesh \mathcal{M} and a filter \mathcal{F} is defined by:

$$(\mathcal{M} * \mathcal{F}) = \sum_r \sum_{\theta} m_{r,\theta} \cdot f_{r,\theta}, \quad (1)$$

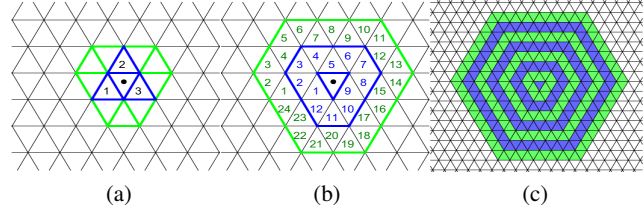


Fig. 1. ORF construction: (a) Three f_{out} facets (in blue) around the central facet f_c are selected, and f_{gap} facets (in green) closes the gap between each pair of them, keeping a clock-wise ordered ring (b), which can be propagated; (c) ORF encompassing 7 rings.

where $m_{r,\theta}$, and $f_{r,\theta}$ are, respectively, a scalar function computed on the mesh and the filter values, both at radius r and angle θ . In images, the convolution is performed at each pixel: neighbor pixels are multiplied by the filter values; in our proposed approach, instead, the convolution is performed on the facets of the mesh, therefore filter values have to be determined at each facet of the ring. In image processing, it is possible to differentiate between *discrete* and *continuous* filters: 1) *discrete filters* are defined and represented by $N \times N$ matrices, as edge detectors, Sobel, *etc.*; 2) *continuous filters*, instead, are generated by continuous functions and quantized to fit a $N \times N$ window. Assuming to have a regular triangular mesh, the number of facets per ring is $r \cdot 12$, where r is the ring number. We distinguish between discrete and continuous filters: for continuous filters, we obtain the exact filter value at each facet by applying the function with polar coordinates; for discrete filters, we adapt the number of values at each ring to the filter size by interpolation and/or sub-sampling.

To provide evidence that our proposed approach makes it possible to reproduce any discrete filter on a mesh manifold, we replicate the Sobel and the sharpen filters. The outcomes of these filters show, respectively, a good edge detection (see Fig. 2a), and an enhancement of any scalar function computed on the mesh (see Fig. 2b). As continuous filter, we chose Gabor. In this case, we have been able to get the $r \cdot 12$ values at each ring r , using the Gabor formula in polar coordinates. Figure 2c shows some Gabor filter responses on the mesh.

LBP on the mesh – The Local Binary Pattern (LBP) has been first proposed as texture descriptor for 2D still images. In its first definition [8], LBP generates a binary sequence for each image pixel (from now on referred to as *central pixel*) analyzing its neighborhood inside a 3×3 window. According to (2), each neighbor pixel value n_k is compared with the central one n_c , assigning 1 to the resulting descriptor if $n_k \geq n_c$, and 0 otherwise, that is:

$$LBP(n_c) = \sum_{k=0}^{m-1} s(n_k - n_c) \cdot 2^k, \quad s(x) = \begin{cases} 1 & x \geq 0 \\ 0 & x < 0 \end{cases} \quad (2)$$

where $s(x)$ is the *step function*. The result of such thresholding is a 8 bits pattern, where each bit is weighted by a

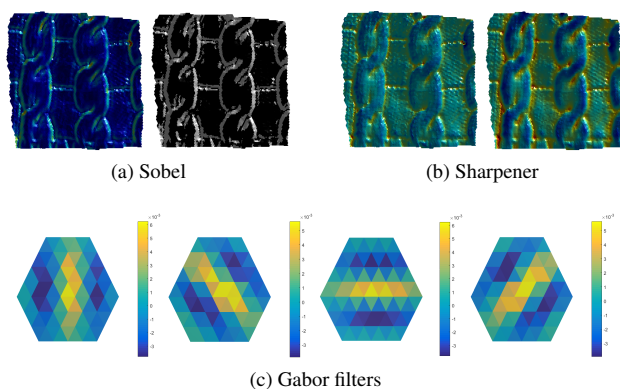


Fig. 2. (a) Convolution of a scalar function on the mesh with the Sobel operator, without and with threshold (on the left and on the right, respectively); (b) The same scalar function on the mesh is enhanced by applying the Sharpen filter; (c) Gabor filter on the mesh using radius quantization 3 and four orientations: 0° , 45° , 90° and 135° from left to right.

power of two according to its position (*i.e.*, the least significant bit is usually assumed to be at the upper left corner of the neighborhood window). Later on, in [17] a multi-resolution and rotation invariant LBP version was presented. The multi-resolution is obtained by computing the LBP across concentric circles, thus introducing the radius r , and sampling pixels m on each circle as new parameters. The rotation invariance is achieved by shifting the binary pattern clockwise till it reaches the minimum value. In the 2D image domain, the LBP computation is simple and efficient thanks to the regular grid structure of the image that naturally defines the neighborhoods and their ordering.

The circular ordering of the facets obtained in the ORF support allows an elegant derivation of a binary pattern (*i.e.*, sequence of 0 and 1 digits) from it, and thus to compute a local binary operator in the same way as in the standard LBP. This solution was first proposed in [9, 10, 11]. While standard LBP compares 8 pixels belonging to a circle of a certain radius around a central pixel, *mesh-LBP* generates a concentric sequence of ring-like patterns around a central facet f_c , whereby facets f_k^r are ordered in a circular fashion in each ring. The *mesh-LBP* is computed as:

$$\text{mesh-LBP}_{r,m}(f_c) = \sum_{k=0}^{m-1} s(h(f_k^r) - h(f_c)) \cdot \alpha(k), \quad (3)$$

where r and m are the ring number and the number of facets per ring, respectively, s is the step function, and $h(f) : \mathcal{M} \rightarrow \mathbb{R}$ is a scalar function defined on the mesh \mathcal{M} (*e.g.*, photometric data or curvature). $\alpha(k)$ is a discrete function, where k represents the facet position. Two functions were defined in the *mesh-LBP*, namely, $\alpha_1(k)=1$ that sums the digits of the pattern, and $\alpha_2(k)=2^k$ that multiplies each digit by a power of 2, as originally proposed in [8].

Based on the above extension of convolution and LBP operators to the mesh domain, in the following, we propose *mesh-LBP* variants as local descriptor for the task of relief patterns analysis and classification on the mesh.

3.1. Mesh-LBP Variants

The potential in using a real 3D support for computing LBP has been investigated in [18, 19], with successful application in 3D face recognition. However, there is much potential in the computational framework offered by the *mesh-LBP* that has not been fully exploited in the basic definition of (3). In fact, similarly to the 2D case, where several LBP variants have been proposed to make the computation more robust to image variations, *e.g.*, noise, or increase the discriminative power, we develop here on the idea of extending the *mesh-LBP* to several variants on the mesh. These variants are based on their 2D counterparts, aiming to transfer most of their properties and analysis capacities to the mesh domain.

Completed Binary Pattern – In [20], *Completed* LBP (CLBP) is designed as combination of binary patterns. CLBP adds more discriminant power to the standard LBP by considering not only the sign of the difference $d_k = n_k - n_c$ in (2) (CLBP-S), but also its magnitude $|d_k|$ (CLBP-M), and central pixel intensity (CLBP-C). CLBP-S/M/C are then combined in different configurations, such as histograms concatenation or multi-dimensional histogram computation. On the mesh, we can follow the same computational approach, thus deriving the *mesh-CLBP-S/M/C* as:

$$\text{mesh-CLBP-M}_{r,m}(f_c) = \sum_{k=0}^{m-1} |(f_k^r, f_c)| \cdot \alpha(k), \quad (4)$$

$$\text{mesh-CLBP-C}_{r,m}(f_c) = s(f_c, \tilde{f}_c), \quad (5)$$

where \tilde{f}_c is the average value among all the central facets f_c of the mesh.

Improved Center-Symmetric Binary Pattern – In [21] the concept of center-symmetric binary pattern (CS-LBP) has been firstly introduced; however such pattern resulted to be strongly dependant to a threshold. To overcome the issue of setting the optimal threshold in the CS-LBP an *Improved CS-LBP* (ICS-LBP) has been proposed in [22, 23]. ICS-LBP compares center symmetric pairs of pixels using the central pixel value as discriminant. Alternatively, it is possible to replace the central pixel with the mean of neighbors values to reduce dependence from noise.

Convolution Binary Pattern – In this family of patterns, the scalar function $h(f)$ in (3) is replaced by the response to a filter. Such response is given by the convolution of the scalar function and a given filter on the mesh as described in (1). The idea of using gradient images in computing LBP was proposed first in [24], where LBP are computed over the magnitude Sobel-gradient image. With our proposed convolution on the mesh paradigm, we extended this concept to dif-

Method		NN	Method	NN
Mesh Convolution	EdgeDetector	99.7%	CMC-1	71.8%
	Sharpen	99.9%	CMC-2	76.3%
	Gabor	99.9%	CMC-3	64.7%
	Sobel	99.3%	KLBO-FV	98.6%
Mesh-LBP Variants	LBP	99.7%	KLBO-SV	97.8%
	ICSLBP	99.6%	edgeLBP-r1	97.9%
	ICSLBP-M	100.0%	edgeLBP-r2	98.6%
	CLBP	99.7%	P/mC/SIFT/FV	95.0%
			T/mC/SIFT/FV	99.3%
		T/VGGConvFV	95.7%	
		T/VGGFC7	98.2%	
		MeshLDSift+FV	99.7%	

Table 1. SHREC’17 relief pattern classification (nearest neighbor (NN) accuracy in percentage): On the left, our proposed Mesh-Convolution filters and Mesh-LBP variants; On the right, comparison with state-of-the-art techniques.

ferent types of discrete and continuous filters including Sobel, Sharpen, Edge Detector, and Gabor.

4. EXPERIMENTATION

The performance of our proposed method has been tested in the task of relief pattern classification, and for geometric texture retrieval, as reported in the following.

Relief Pattern Classification: The scans released in the SHREC’17 track on “Retrieval of surfaces with similar relief pattern” [12] have been used. They are given as meshes (720 in total) with various textile patches as captured by a 3D scanner. Each patch is acquired multiple times for different poses and shape deformations. We adhered to the SHREC’17 competition protocol, whereby the classification performance is evaluated via a 720×720 matrix of mutual distances between all the dataset samples, using Nearest Neighbor (NN) as pattern classifier. The framework parameters have been set as follows: Radius $r=14$ rings, which resulted to be the most effective in covering the largest patterns in the dataset; Samples per ring $m=12$ to be coherent with the first ring (see Fig. 1b); *Local Depth (LD)* as scalar function. The *LD* value is defined as the algebraic distance between the point on the manifold and a reference plane; such plane is determined by the neighborhood vertices (*i.e.*, those in the ORF with radius r), passing from their center of mass, and having the least eigenvector of their covariance matrix as normal. *LD* is our newly proposed feature, which shows great potential in representing the depth information of local regions on mesh manifolds.

In Table 1, on the left, we show the results obtained with the convolution filters and mesh-LBP variants (plus the standard one), computed on the mesh manifold using our technique. In terms of *NN* accuracy, all the proposed descriptors perform very well electing *Gabor* and *Sharpen* as best mesh convolution filter with 99.9% accuracy, and *Mesh-ICSLBP-M* as best Mesh-LBP variant with an outstanding 100%. On the right, instead, we report results for state-of-the-art techniques.

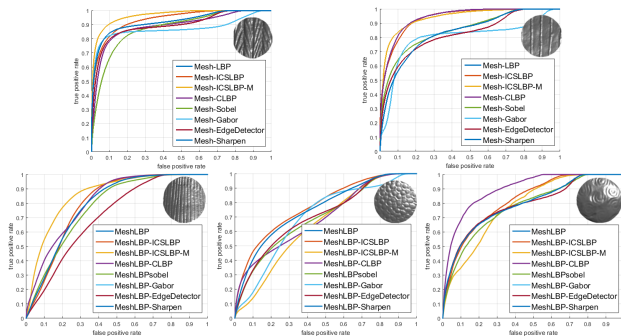


Fig. 3. SHREC’18 geometric texture retrieval: ROC curves of Mesh-Convolution filters and Mesh-LBP variants.

An additional relevant aspect of our approach lies on its linear complexity. Among the methods listed in Table 1, only *edgeLBP* [15] is able to extract the feature directly from the mesh manifold like we do, but with a $O(n^2)$ complexity.

Geometric Texture Retrieval: This work referred explicitly to the SHREC’18 dataset (track on “Recognition of geometric patterns over 3D models”) that includes scans of archaeological artifacts with geometric texture on the surface. We tested our technique on such dataset, proposing, to the best of our knowledge, the first retrieval results on such challenging set of scans. We identified 8 scans showing one or more geometric textures on their surface, and manually annotated them by selecting areas with different geometric textures. This resulted in 5 different texture patches. In Fig. 3, we report the ROC curves the five different texture patterns. The mesh-ICSLBP-M achieved again the best performance with an average normalized Area Under the (ROC) Curve (*AUC*) of 0.84.

5. CONCLUSION

In this paper, we presented a versatile framework for relief pattern analysis, classification and retrieval on mesh manifolds. Exploiting the potentials of ORF, we first propose a framework, which enables convolution operation on mesh manifolds. To demonstrate its flexibility, discrete (Sobel, edge detector, sharpen) and continuous (Gabor) convolution filters have been defined and applied directly on the mesh. The same framework has been also used to develop several mesh-LBP variants retracing the success of 2D LBP in the 3D domain.

Convolution filters and mesh-LBP variants have been tested and compared to the most recent state-of-the-art techniques on the SHREC’17 dataset for relief pattern classification. All our descriptors show remarkable results, outperforming previous methods: in particular *Mesh-ICSLBP-M* obtained perfect accuracy with *NN* classification. Finally, we propose the first results on the SHREC’18 dataset for the challenging task of geometric texture retrieval.

6. REFERENCES

- [1] Johan W. Tangelder and Remco C. Veltkamp, "A survey of content based 3d shape retrieval methods," *Multimedia Tools and Applications*, vol. 39, no. 3, pp. 441–471, Sept. 2008.
- [2] Ahlem Othmani, Lew F.C. Lew Yan Voon, Christophe Stolz, and Alexandre Piboule, "Single tree species classification from terrestrial laser scanning data for forest inventory," *Pattern Recognition Letters*, vol. 34, no. 16, pp. 2144–2150, 2013.
- [3] Matthias Zeppelzauer, Georg Poier, Markus Seidl, Christian Reinbacher, Samuel Schuster, Christian Breiteneder, and Horst Bischof, "Interactive 3d segmentation of rock-art by enhanced depth maps and gradient preserving regularization," *J. Comput. Cult. Herit.*, vol. 9, no. 4, pp. 19:1–19:30, Sept. 2016.
- [4] Xianfang Sun, Paul L Rosin, Ralph R Martin, and Frank C Langbein, "Bas-relief generation using adaptive histogram equalization," *IEEE Trans. on Visualization and Computer Graphics*, vol. 15, no. 4, pp. 642–653, 2009.
- [5] M. Wei, Y. Tian, W. M. Pang, C. C. L. Wang, M. Y. Pang, J. Wang, J. Qin, and P. A. Heng, "Bas-relief modeling from normal layers," *IEEE Trans. on Visualization and Computer Graphics*, to appear 2018.
- [6] F. Liu and R. W. Picard, "Periodicity, directionality, and randomness: Wold features for image modeling and retrieval," *IEEE Trans. on Pattern Analysis and Machine Intelligence*, vol. 18, no. 7, pp. 722–733, Jul 1996.
- [7] Chien-Chang Chen and Daniel C. Chen, "Multi-resolutional gabor filter in texture analysis," *Pattern Recognition Letters*, vol. 17, no. 10, pp. 1069 – 1076, 1996.
- [8] Timo Ojala, Matti Pietikäinen, and David Harwood, "A comparative study of texture measures with classification based on featured distributions," *Pattern Recognition*, vol. 29, no. 1, pp. 51–59, jan 1996.
- [9] Naoufel Werghi, Stefano Berretti, and Alberto Del Bimbo, "The mesh-lbp: a framework for extracting local binary patterns from discrete manifolds," *IEEE Trans. on Image Processing*, vol. 24, no. 1, pp. 220–235, 2015.
- [10] Naoufel Werghi, Claudio Tortorici, Stefano Berretti, and Alberto Del Bimbo, "Representing 3D texture on mesh manifolds for retrieval and recognition applications," in *2015 IEEE Conference on Computer Vision and Pattern Recognition (CVPR)*, jun 2015, vol. 07-12-June, pp. 2521–2530, IEEE.
- [11] Naoufel Werghi, Claudio Tortorici, Stefano Berretti, and Alberto del Bimbo, "Local binary patterns on triangular meshes: Concept and applications," *Computer Vision and Image Understanding*, vol. 139, pp. 161–177, oct 2015.
- [12] Silvia Biasotti, E. Moscoso Thompson, M. Aono, A. Ben Hamza, B. Bustos, S. Dong, B. Du, Amin Fehri, H. Li, F. A. Limberger, M. Masoumi, M. Rezaei, Ivan Sipiran, L. Sun, A. Tatsuma, S. Velasco Forero, R. C. Wilson, Y. Wu, J. Zhang, T. Zhao, F. Fornasa, A. Giachetti, Santiago Velasco-Forero, R. C. Wilson, Y. Wu, Y. Zhang, T. Zhao, F. Fornasa, and A. Giachetti, "Shrec'17 Track: Retrieval of surfaces with similar relief patterns," apr 2017.
- [13] Frederico A. Limberger and Richard C. Wilson, "Feature encoding of spectral signatures for 3d non-rigid shape retrieval," in *British Machine Vision Conf.*, pp. 1–13.
- [14] A. Giachetti, "Effective Characterization of Relief Patterns," *Computer Graphics Forum*, vol. 37, no. 5, pp. 83–92, aug 2018.
- [15] Elia Moscoso Thompson and Silvia Biasotti, "Description and retrieval of geometric patterns on surface meshes using an edge-based LBP approach," *Pattern Recognition*, vol. 82, pp. 1–15, oct 2018.
- [16] Naoufel Werghi, Mohamed Rahayem, and Johan Kjellander, "An ordered topological representation of 3D triangular mesh facial surface: concept and applications," *EURASIP Journal on Advances in Signal Processing*, vol. 2012, no. 1, pp. 144, 2012.
- [17] Timo Ojala, M. Pietikäinen, and T. Maenpaa, "Multiresolution gray-scale and rotation invariant texture classification with local binary patterns," *IEEE Transactions on Pattern Analysis and Machine Intelligence*, vol. 24, no. 7, pp. 971–987, jul 2002.
- [18] Naoufel Werghi, Claudio Tortorici, Stefano Berretti, and Alberto Del Bimbo, "Boosting 3D LBP-Based Face Recognition by Fusing Shape and Texture Descriptors on the Mesh," *IEEE Transactions on Information Forensics and Security*, vol. 11, no. 5, pp. 964–979, may 2016.
- [19] Claudio Tortorici, Naoufel Werghi, and Stefano Berretti, "Boosting 3D LBP-based face recognition by fusing shape and texture descriptors on the mesh," in *2015 IEEE International Conference on Image Processing (ICIP)*, sep 2015, pp. 2670–2674, IEEE.
- [20] Zhenhua Guo, Lei Zhang, and David Zhang, "A Completed Modeling of Local Binary Pattern Operator for Texture Classification," *IEEE Transactions on Image Processing*, vol. 19, no. 6, pp. 1657–1663, jun 2010.
- [21] Marko Heikkilä, Matti Pietikäinen, and Cordelia Schmid, "Description of interest regions with local binary patterns," *Pattern Recognition*, vol. 42, no. 3, pp. 425–436, mar 2009.
- [22] Xiaosheng Wu and Junding Sun, "An Effective Texture Spectrum Descriptor," in *2009 Fifth International Conference on Information Assurance and Security*, 2009, vol. 2, pp. 361–364, IEEE.
- [23] Sun Junding, Zhu Shisong, and Wu Xiaosheng, "Image retrieval based on an improved CS-LBP descriptor," *2010 2nd IEEE International Conference on Information Management and Engineering*, pp. 115–117, 2010.
- [24] S Moore and R Bowden, "Local binary patterns for multi-view facial expression recognition," *Computer Vision and Image Understanding*, vol. 115, pp. 541–558, 2011.